Available online at www.sciencedirect.com
SCIENCE DIRECT®
Precambrian Research 125 (2003) 179–189
Precambrian Research
www.elsevier.com/locate/precamres

Geochronological and isotopic constraints on the Mesoproterozoic Namaqua–Natal Belt: evidence from deep borehole intersections in South Africa

B.M. Eglington [a,*], R.A. Armstrong [b]

[a] *Department of Geology, University of Saskatchewan, 114 Science Place, Saskatoon, Sask., Canada S7N 5E2*
[b] *Research School of Earth Sciences, Australian National University (ANU), Canberra, Australia*

Received 22 December 2000; accepted 29 October 2002

Abstract

Mesoproterozoic lithologies of the Namaqua–Natal Belt are exposed in the west and east of South Africa but the central section of the belt is obscured by younger sedimentary cover. This belt is one of several Grenvillian-aged belts world-wide and is of importance in reconstructions of the Meso- to Neo-Proterozoic supercontinent of Rodinia.

Zircons from granite and biotite gneiss in two deep boreholes which penetrated the Phanerozoic cover provide SHRIMP U–Pb dates of $1053^{+29}/_{-25}$ Ma and $1134^{+15}/_{-15}$ Ma. Sm–Nd model dates for whole-rock samples from these and two other boreholes range from ~2400 to 1200 Ma, unlike model dates from the eastern (Natal) sector of the Namaqua–Natal Belt which are all younger than ~1400 Ma. Model dates are similar to those noted in the Bushmanland and Richtersveld Sub-provinces of the western (Namaqua) sector of the Belt. The results are interpreted to indicate that this Proterozoic crust may be an easterly extension of the Bushmanland Sub-province or some equivalent terrane and that there must be a terrane boundary between the eastern-most borehole studied and the surface outcrops further east.

Keywords: Mesoproterozoic; Namaqua–Natal; Isotope; Geochronology; South Africa

1. Introduction

The Namaqua–Natal Belt is situated along the southern and south western margin of the Archaean Kaapvaal Craton. The Belt can also be followed north-west to the Awasib Mountain Terrane of southern Namibia (Hoal et al., 1989), whilst continental reconstructions place the Falkland Islands, Agulhas Plateau and the Maudheim Province of Antarctica to the east (Allen and Tucholke, 1981; Grantham et al., 1988; Thomas et al., 2000). This belt and its postulated extensions, are thought to form part of a greater network of Mesoproterozoic (Grenvillian-aged) belts which have been used to help define the configuration of the Meso- to Neo-Proterozoic supercontinent, Rodinia.

Mesoproterozoic dates (~1000–1300 Ma) have been obtained from basement exposures in the west (Namaqua sector: Kheis, Gordonia and Bushmanland Sub-provinces) and east (Natal sector) of the Namaqua–Natal Belt (Nicolaysen and Burger, 1965; Barton, 1983; Eglington et al., 1989; Thomas and Eglington, 1990; Thomas et al., 1993; Clifford et al., 1995; Robb et al., 1999), but the central portion of the Belt is obscured by Phanerozoic cover (Fig. 1).

* Corresponding author.
E-mail address: bruce.eglington@usask.ca (B.M. Eglington).

0301-9268/$ – see front matter © 2002 Elsevier B.V. All rights reserved.
PII: S0301-9268(02)00199-7

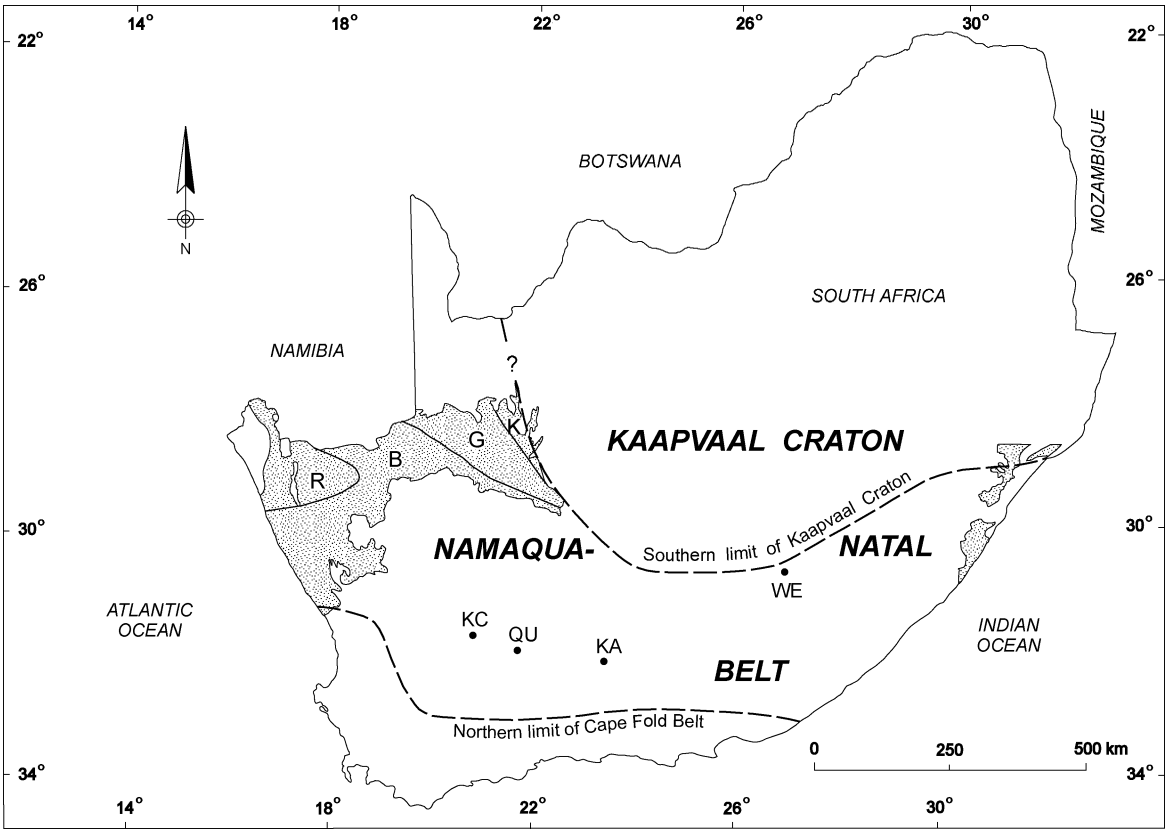

Fig. 1. Locality map for boreholes KC 1/70, QU 1/65, KA 1/66 and WE 1/66 relative to exposures of the Proterozoic Namaqua–Natal Belt (stippled), the Archaean Kaapvaal Craton and the Phanerozoic Cape Fold Belt. Sub-provinces within the Namaqua sector of the Namaqua–Natal Belt are labelled as follows: B, Bushmanland; G, Gordonia; K, Kheis; R, Richtersveld.

Palaeoproterozoic (~1800–2000 Ma) dates have been recorded from several sections of the Namaqua sector of the Belt (Reid, 1997) but are absent from the Natal sector.

Several boreholes were drilled into the Karoo Supergroup during the 1960s as part of regional exploration efforts for oil (Winter and Venter, 1970). Some of these penetrated the Phanerozoic cover lithologies and encountered various basement granitoids and gneisses (Fig. 1). Bulk population zircon model $^{207}Pb/^{206}Pb$ dates of ~1000 Ma have been reported for zircons from some of these intersections (QU 1/65 ~1059 Ma, KA 1/66 ~838 Ma and WE 1/66 ~1029 Ma; Burger and Coertze, 1973), confirming the link between the western and eastern Namaqua–Natal exposures.

The present paper documents the results of precise dating of lithologies from two of the boreholes (QU 1/65 and WE 1/66), together with Rb–Sr and Sm–Nd isotope analyses of whole-rock powders of five samples from four of the boreholes (KA 1/66, KC 1/70, QU 1/65 and WE 1/66). The rocks concerned range from granitoids to biotite gneiss (Table 3).

2. Analytical procedures

Rb–Sr and Sm–Nd isotope techniques utilised for this study followed those previously documented (Harmer et al., 1998). Model $^{Nd}T_{DM}$ dates have been calculated using the 1991 DePaolo model for depleted mantle (DePaolo et al., 1991).

Zircon separates for this study were taken from previously prepared concentrates in the collection of heavy minerals processed and analysed at the National

Physical Research Laboratory (NPRL), CSIR, South Africa, mostly by Burger and coworkers (Nicolaysen and Burger, 1965; Burger and Coertze, 1973). This collection houses samples used in the dating of southern African lithologies since the late 1950s and is now housed at the Council for Geoscience, Pretoria, South Africa.

Representative aliquots of each zircon fraction were mounted in epoxy at the Research School of Earth Sciences, Australian National University (ANU) together with the zircon standards SL13 and AS3. Populations were characterised using transmitted and reflected light, back-scatter electron imaging and cathodoluminescence imaging, the latter two techniques on the SEM at the electron microscopy unit at ANU. Analyses were performed on SHRIMP I and II. Spots for analysis were selected on the basis of the optical and cathodoluminescence images obtained prior to analysis.

Analysis on SHRIMP and subsequent data reduction were performed following previously documented techniques (Compston et al., 1984; Claoue-Long et al., 1995). U/Pb in the unknowns were normalised to a $^{206}Pb^*/^{238}U$ value of 0.1859, equivalent to an age of 1099.1 Ma for AS3. U and Th concentrations were determined relative to those measured in the SL13 standard.

Correction for common lead was made using the measured $^{204}Pb/^{206}Pb$ ratio and model common-lead ratios (Cumming and Richards, 1975). Unless otherwise stated, dates are based on $^{207}Pb^*/^{206}Pb^*$ ratios and an assessment of the concordance of the data and were calculated using recommended decay constants (Steiger and Jäger, 1977). Dates and model ratios have been calculated using Geodate for Windows (Eglington and Harmer, 1999), a Windows'95 implementation of previously described techniques (Eglington and Harmer, 1993; Ludwig, 1998). Uncertainties in the SHRIMP U–Pb results tables and plots are at 1 sigma whilst weighted averages and interpreted dates are quoted with 95% confidence uncertainties. Model Rb–Sr and Sm–Nd dates and epsilon values are quoted at 95% confidence levels.

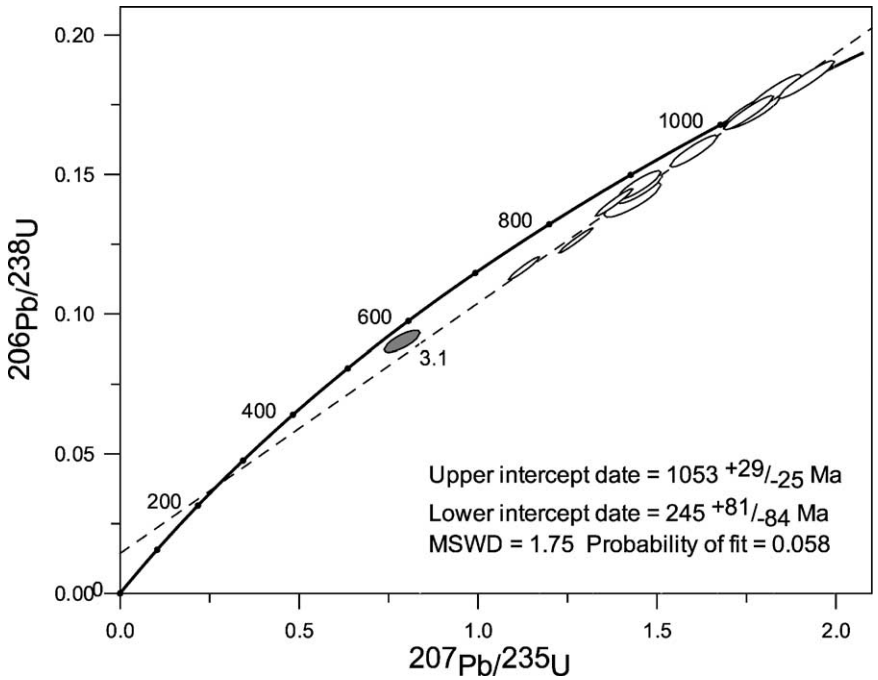

Fig. 2. Wetherill U–Pb plot for SHRIMP zircon analyses of megacrystic granite from borehole QU 1/65. Spot 3.1 is excluded from the regression result shown.

Table 1
Summary of SHRIMP U–Pb zircon results for sample Zr69027 from borehole QU 1/65

Grain. Spot	U (ppm)	Th (ppm)	Th/U	Pb* (ppm)	$^{204}Pb/^{206}Pb$	f_{206} (%)	Radiogenic ratios						Ages (Ma)						Conc. (%)
							$^{206}Pb/^{238}U$	±	$^{207}Pb/^{235}Pb$	±	$^{207}Pb/^{206}Pb$	±	$^{206}Pb/^{238}U$	±	$^{207}Pb/^{235}Pb$	±	$^{207}Pb/^{206}Pb$	±	
1.1	892	159	0.178	149	0.000054	0.092	0.1721	0.0050	1.756	0.057	0.0740	0.0008	1024	28	1029	21	1041	22	98
2.1	889	165	0.185	110	0.000039	0.066	0.1264	0.0036	1.274	0.038	0.0731	0.0005	767	21	834	17	1017	12	75
3.1	1347	115	0.086	118	0.002136	3.606	0.0903	0.0032	0.788	0.041	0.0633	0.0021	557	19	590	24	718	74	78
4.1	698	249	0.357	104	0.001100	1.864	0.1448	0.0042	1.452	0.051	0.0728	0.0012	871	24	911	21	1007	34	87
5.1	813	87.6	0.108	114	0.000390	0.659	0.1462	0.0042	1.450	0.050	0.0719	0.0011	879	24	910	21	984	32	89
5.2	265	115	0.434	49	0.000143	0.241	0.1795	0.0052	1.829	0.060	0.0739	0.0009	1064	29	1056	22	1039	25	102
6.1	148	52.5	0.355	26	0.000051	0.087	0.1728	0.0053	1.767	0.067	0.0742	0.0014	1027	29	1034	25	1047	38	98
7.1	843	269	0.319	96	0.000211	0.355	0.1164	0.0034	1.129	0.035	0.0703	0.0006	710	19	767	17	938	17	76
8.1	349	152	0.435	58	0.000122	0.206	0.1584	0.0047	1.603	0.054	0.0734	0.0010	948	26	971	21	1025	28	92
9.1	165	105	0.639	33	0.000072	0.122	0.1840	0.0055	1.918	0.064	0.0756	0.0008	1089	30	1087	22	1084	22	101
10.1	257	156	0.605	40	0.000350	0.594	0.1409	0.0051	1.432	0.065	0.0737	0.0017	850	29	902	28	1033	48	82
11.1	1091	67	0.06	143	0.000133	0.225	0.1400	0.0040	1.380	0.042	0.0715	0.0006	845	23	881	18	972	16	87

Uncertainties given at the one σ level. f_{206} (%) denotes ^{206}Pb that is common Pb. Correction for common Pb made using that measured $^{204}Pb/^{206}Pb$ ratio. For conc. (%), 100% denotes a concordant analysis.

Table 2
Summary of SHRIMP U–Pb zircon results for sample Zr69037 from borehole WE 1/66

Grain. Spot	U (ppm)	Th (ppm)	Th/U	Pb* (ppm)	$^{204}Pb/^{206}Pb$	f_{206} (%)	Radiogenic ratios						Ages (Ma)						Conc. (%)
							$^{206}Pb/^{238}U$	±	$^{207}Pb/^{235}Pb$	±	$^{207}Pb/^{206}Pb$	±	$^{206}Pb/^{238}U$	±	$^{207}Pb/^{235}Pb$	±	$^{207}Pb/^{206}Pb$	±	
1.1	123.1	49	0.399	26	0.000313	0.53	0.2059	0.0063	2.127	0.082	0.0749	0.0015	1207	34	1157	27	1066	41	113
2.1	199.5	76	0.383	39	0.000024	0.04	0.1870	0.0056	2.036	0.070	0.0790	0.0011	1105	30	1128	24	1171	27	94
3.1	140.3	61	0.434	30	0.000144	0.24	0.2059	0.0066	2.186	0.086	0.0770	0.0015	1207	35	1177	28	1121	40	108
4.1	195.1	87	0.448	43	0.000062	0.11	0.2128	0.0067	2.279	0.080	0.0777	0.0009	1244	36	1206	25	1139	23	109
4.2	88.55	47	0.528	20	0.000141	0.24	0.2089	0.0070	2.213	0.104	0.0768	0.0022	1223	38	1185	33	1117	58	110
5.1	189.8	90	0.476	40	0.000170	0.29	0.1987	0.0064	2.080	0.078	0.0759	0.0011	1169	35	1142	26	1093	31	107
6.1	171.2	72	0.418	36	0.000083	0.14	0.2033	0.0063	2.168	0.075	0.0773	0.0009	1193	34	1171	24	1129	24	106
7.1	157.9	54	0.344	30	0.000100	0.17	0.1845	0.0093	1.941	0.104	0.0763	0.0010	1092	51	1095	37	1102	27	99
8.1	117.8	47	0.396	24	0.000122	0.21	0.1994	0.0065	2.153	0.084	0.0783	0.0014	1172	35	1166	27	1155	36	102
9.1	142.6	60	0.424	30	0.000067	0.11	0.2004	0.0064	2.168	0.081	0.0785	0.0013	1177	34	1171	26	1159	33	102
10.1	219.8	99	0.452	47	0.000140	0.24	0.2056	0.0062	2.195	0.076	0.0774	0.0011	1205	33	1179	24	1132	27	107
11.1	238.4	68	0.284	48	0.000118	0.20	0.2009	0.0062	2.120	0.077	0.0766	0.0012	1180	33	1156	25	1110	31	106
12.1	228.1	86	0.379	42	0.000167	0.28	0.1781	0.0056	1.888	0.067	0.0769	0.0010	1057	31	1077	24	1118	27	95
13.1	295.3	146	0.495	61	0.000175	0.30	0.1946	0.0059	2.117	0.071	0.0789	0.0009	1146	32	1155	23	1171	23	98
14.1	315.3	140	0.445	62	0.000036	0.06	0.1883	0.0055	2.022	0.066	0.0779	0.0009	1112	30	1123	22	1144	23	97
15.1	199	89	0.44	41	0.000034	0.06	0.1976	0.0061	2.135	0.076	0.0784	0.0011	1162	33	1160	25	1156	28	101

Uncertainties given at the one σ level. f_{206} (%) denotes the percentage of ^{206}Pb that is common Pb. Correction for common Pb made using the measured $^{204}Pb/^{206}Pb$ ratio. For conc. (%), 100% denotes a concordant analysis.

3. Results

SHRIMP U–Pb results for zircons from boreholes QU 1/65 and WE 1/66 are provided in Tables 1 and 2 whilst Rb–Sr and Sm–Nd isotope results for powdered whole-rock samples from boreholes QU 1/65, KC 1/70, KA 1/66 and WE 1/66 are provided in Table 3.

The U–Pb data for QU 1/65 define a discordia array on a Wetherill type plot (Fig. 2). Regression of all the data, assuming a multi-episodic model to explain scatter beyond analytical uncertainties (MSWD = 1.8), provides an upper intercept date of $1061^{+56}/_{43}$ Ma. Omission of the analysis exhibiting most lead loss (spot 3.1) permits calculation of a normally weighted regression line with an upper intercept date of $1053^{+29}/_{-25}$ Ma (MSWD = 1.75, probability of fit = 0.058). The lower intercept date of $245^{+81}/_{-84}$ Ma is similar to ages expected for activity associated with the Cape Fold Belt. The position of spot 3.1 above the best-fit line may indicate that the zircons from granite in borehole QU 1/65 were affected by lead loss associated with Pan African overprinting as well as by more recent lead loss. The date of ~1053 Ma is interpreted as the emplacement age of the megacrystic granitoid present in this borehole. This megacrystic granite is presumably a correlative of the ~1.06 Ga Spektakel Suite megacrystic granites of the Namaqua sector of the belt (Thomas et al., 1996; Robb et al., 1999) and of the 1.06–1.03 Ga Oribi Gorge Suite megacrystic granitoids in the Natal sector (Thomas et al., 1993).

All spots analysed from sample WE 1/66 cluster close to concordia (Fig. 3) but the spread in Pb/U ratios precludes calculation of a concordia date (Ludwig, 1998). The weighted average model $^{207}Pb/^{206}Pb$ date for all the spots analysed from this

Table 3
Rb–Sr and Sm–Nd isotopic data for basement samples from four boreholes which penetrate Phanerozoic cover in southern Africa

	Borehole				
	QU 1/65		KA 1/66	KC 1/70	WE 1/66
	Depth (m)				
	2493	2993	2579	6005	3735
Lithology	Megacrystic granite	Biotite granodioritic gneiss	Dark grey microporphyry	Granitoid gneiss	Biotite gneiss
Rb	223.8	42.44	16.72	52.67	542.9
Sr	160.6	657.6	34.45	46.78	9.64
$^{87}Rb/^{86}Sr$	4.057	0.1869	1.409	3.268	193.9
$^{87}Rb/^{86}Sr$	0.772224 ± 14	0.708909 ± 14	0.741676 ± 13	0.739391 ± 20	2.651 ± 9
1 sigma errors (%)	0.8, 0.02	0.8, 0.01	0.8, 0.01	0.8, 0.02	0.8, 0.05
Sm	14.90	3.611	1.357	0.7174	2.646
Nd	73.20	19.94	6.372	3.030	10.36
$^{147}Sm^{144}Nd$	0.1231	0.1095	0.1287	0.1431	0.1544
$^{143}Nd^{144}Nd$	0.512327 ± 10	0.511447 ± 10	0.511687 ± 8	0.512267 ± 12	0.512143 ± 13
1 sigma errors (%)	0.6, 0.006	0.6, 0.006	0.6, 0.006	0.6, 0.006	0.6, 0.006
ε_{Nd} (T)	+3.8	−10.5	−8.6	0.0	−3.6
T (Ma)	1053	1150	1150	1150	1134
$^{Nd}T_{DM}$ (Ma)	1199 ± 116	2326 ± 87	2427 ± 96	1662 ± 130	2307 ± 126

Rb, Sr determined following standard dissolution and extraction on cation columns. NIST 987 = 0.71028 ± 19. 1 sigma analytical errors given in percent and refer to $^{87}Rb/^{86}Sr$ and $^{87}Sr/^{86}Sr$, respectively.

Sm, Nd determined following microwave autoclave dissolution and extraction with standard cation and HDEHP on teflon ion exchange techniques. Johnson Matthey standard = 0.511783 ± 2, equivalent to a value of 0.511820 for La Jolla standard. BCR-1 Sm = 6.58, Nd = 28.7, $^{143}Nd/^{144}Nd$ = 0.51264 ± 2.1 sigma analytical errors given in percent and refer to $^{147}Sm/^{144}Nd$ and $^{143}Nd/^{144}Nd$, respectively. $^{Nd}T_{DM}$ determined using the GEODATE for Windows software (Eglington and Harmer, 1999) and based on the depleted mantle model of DePaolo et al. (1991). Errors are 95% confidence.

ε_{Nd} are based on values of 0.1967 and 0.51264 for $^{147}Sm/^{144}Nd$ and $^{143}Nd/^{144}Nd$, respectively, in CHUR.

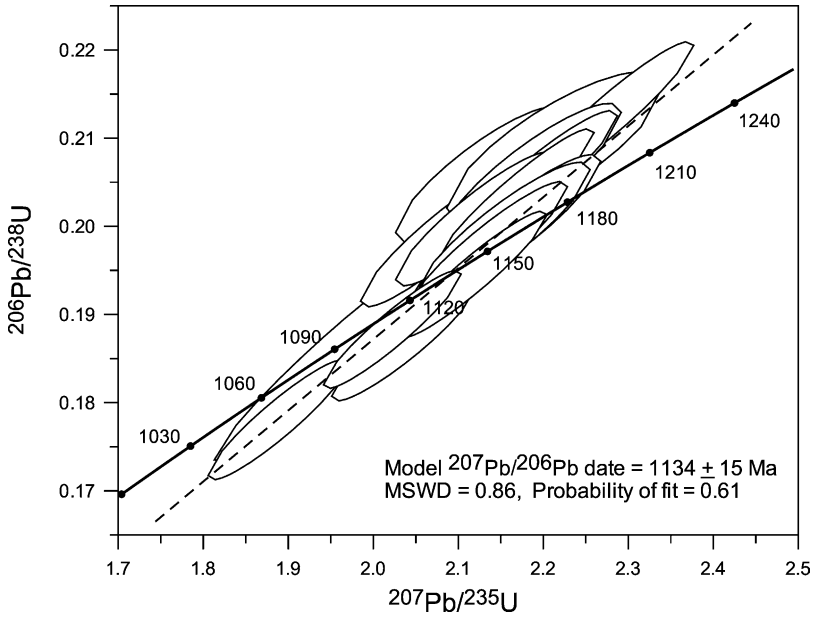

Fig. 3. Wetherill concordia plot illustrating the concordant nature of the spots analysed from borehole WE 1/66. The data define a weighted average $^{207}Pb/^{206}Pb$ date of 1134 ± 15 Ma.

sample is $1134^{+15}/_{-15}$ Ma (MSWD = 0.86, probability of fit = 0.61) and this date is deemed to represent the age of formation of the precursor to what is now a biotite gneiss.

Model $^{Nd}T_{DM}$ dates for the five samples analysed range from ~1.2 Ga for the megacrystic granite in borehole QU 1/65 to ~2.4 Ga (Table 3). The biotite gneiss from borehole WE 1/66, dated at $1134^{+15}/_{-15}$ Ma, provides a $^{Nd}T_{DM}$ date of ~2.4 Ga (Table 3). Epsilon values for the samples range from +3.8 for the megacrystic granite in borehole QU 1/65 to −10.5 (Table 3).

4. Discussion

Dates for emplacement and extrusion of the various magmatic components of the different sub-provinces and terranes comprising the Namaqua–Natal Belt are illustrated in Fig. 4. Four main periods of activity are evident: at ~1.8 to 2 Ga, ~1.2 Ga, ~1.15 Ga and ~1.06 Ga. The two new zircon dates reported in this paper coincide with two of these dominant periods of magmatic activity within the belt (~1.15 Ga in the case of WE 1/66 and ~1.06 Ga for megacrystic granite from QU 1/65) and relate to the early and late phases of late Mesoproterozoic igneous activity within the belt.

The geochronological and isotopic evolution of crust in the Namaqua–Natal Belt is dominated by mantle extraction events at ~2 and 1.4 Ga (Rogers and Hawkesworth, 1982; Barton, 1983; Eglington et al., 1989; Thomas and Eglington, 1990; Thomas et al., 1993; Clifford et al., 1995; Reid, 1997; Reid et al., 1997; Wareham et al., 1998; Robb et al., 1999; and references quoted therein). This two-stage evolution is well illustrated on plots of initial $^{87}Sr/^{86}Sr$ relative to date (Fig. 5) and of epsilon Nd relative to date (Fig. 6).

Isotopic data from the Namaqua sector of the Province define two trends on a plot of initial $^{87}Sr/^{86}Sr$ versus date (Barton, 1983; Eglington et al., 1989; Fig. 5), both having increasing initial $^{87}Sr/^{86}Sr$ with decreasing age. The one trend intersects model "bulk earth" and "depleted mantle" at about 1.9 Ga, whilst the other intersects these model curves at about 1.4 Ga. Intrusions which define the older vector are from the Richtersveld and Bushmanland Sub-provinces, whereas the younger trend includes intrusive lithologies from the Gordonia Sub-province, and some of the younger intrusions from the Bushmanland Sub-province. In contrast to the situation in

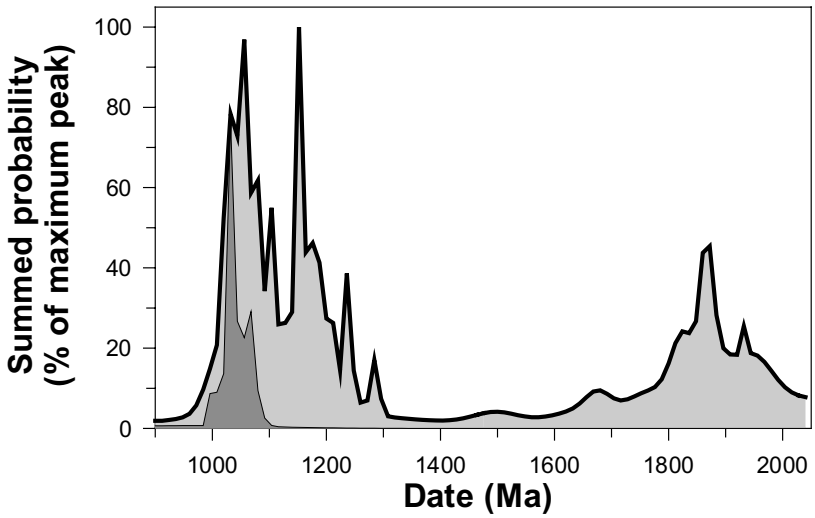

Fig. 4. Summed probability distribution of dates from the Namaqua–Natal Belt, classified according to interpreted relevance of each date. Extrusion and emplacement dates are shown in light stipple and dates reflecting growth of metamorphic zircon are in a dark stipple. Sources of data are given in the text and supplemented by unpublished data of the authors and co-workers at the Council for Geoscience. All peaks have been normalised to a value of 100% for the major peak.

the Namaqua sector of the belt, the Natal data fall only within the trend for ~1400 Ma protolith development, equivalent to that of the Gordonia Sub-province to the west (Eglington et al., 1989; Fig. 5). Model epsilon Nd values from the Namaqua–Natal Belt also delineate two development fields, one for a ~2 Ga protolith and the other for a ~1.4 Ga protolith (Fig. 6). Epsilon Nd values for the samples analysed seemingly fall into two groups with the granitoid samples from boreholes QU 1/65 (2493 m) and KC 1/70 plotting in the crustal development field for ~1.4 Ga mantle extraction whilst the other samples suggest reworking of older, originally ~2 Ga protoliths (Fig. 6).

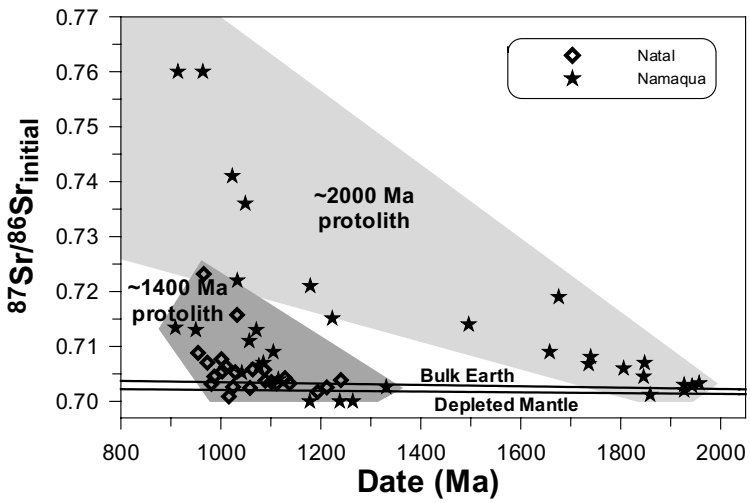

Fig. 5. Plot of apparent date vs. $^{87}Sr/^{86}Sr$ initial ratio for units from the Namaqua and Natal sectors of the Namaqua–Natal Belt. Sources of data are referenced in the text.

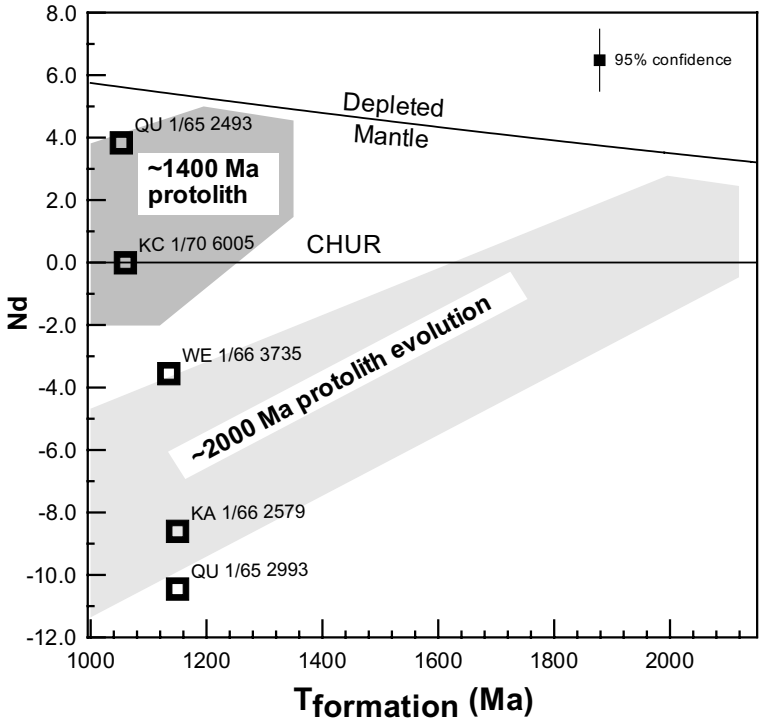

Fig. 6. Plot of ε_{Nd} relative to formation age for samples from the four boreholes relative to the evolution fields for the ~2 and 1.4 Ga protoliths identified elsewhere in the Namaqua–Natal belt.

Model Nd dates from the Namaqua–Natal Belt support the $^{87}Sr/^{86}Sr$ and ε_{Nd} interpretation with two distinct peaks on an histogram of $^{Nd}T_{DM}$ dates for the Namaqua sector (at ~2.2 and 1.5 Ga, Fig. 7) whilst the Natal data exhibit younger peaks (at ~1.4 and 1.6 Ga, Fig. 7). Sm–Nd isotope data for granulite xenoliths from kimberlites in northern Lesotho have provided similar results to the Natal data (Rogers and Hawkesworth, 1982).

These different peaks have been interpreted as representing the time at which significant proportions of crustal material were extracted from the mantle. In both Natal and southern Namibia, the sequence of dates can be correlated with a lithological progression from basaltic volcanics to calc-alkaline tonalites and granodiorites to younger granites (Eglington et al., 1989; Hoal et al., 1989; Thomas and Eglington, 1990). This has been interpreted by these authors as reworking of originally oceanic type material, possibly initially in an island arc type environment, followed by plate accretion and the genesis of granites which exhibit A-type chemical signatures.

The $^{Nd}T_{DM}$ dates obtained from the sub-Karoo intersections are generally older than those obtained for supracrustal gneisses and intrusive granitoids from the Cape Meredith Complex, Falkland Islands (Thomas et al., 2000). Rodinian reconstructions suggest that the Falkland Islands were situated east of South Africa at a latitude similar to that of the samples reported here (African framework for the reconstruction) (Jacobs et al., 1999; Wareham et al., 1998). If these reconstructions are correct, then the older protolith evident in the Bushmanland Sub-province of Namaqualand and the sub-Karoo boreholes must terminate before reaching either the Mesoproterozoic exposures in Natal or the reconstructed position of the Cape Meredith Complex.

The data presented here provide further evidence for the delineation of isotopically distinct terranes. Whilst some of these terranes formed in the early Proterozoic (~2 Ga), others formed much later. Terrane accretion occurred after this latter period of juvenile crust

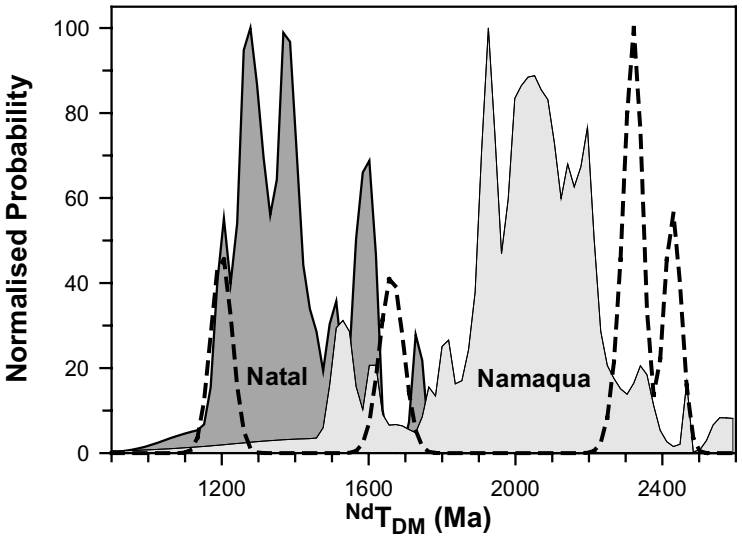

Fig. 7. Probability plot of $^{Nd}T_{DM}$ model dates for lithologies from the Namaqua and Natal sectors of the Namaqua–Natal Belt compared with results obtained for the samples reported here (heavy dashed line). Note that the scarcity of younger model dates from the Namaqua sector is, in part, a function of sample bias in that the areas for which Sr isotope data suggest juvenile additions have not been analysed for Nd isotopes.

addition at ~1.1–1 Ga. Future reconstructions of Rodinia will need to take into account the variability produced by the accretion of isotopically distinct terranes such as those illustrated here for southern Africa.

5. Conclusions

U–Pb dating of zircons from two boreholes which intersected basement beneath the Phanerozoic Karoo lithologies of southern Africa provide precise Proterozoic dates which are consistent with the two main periods of Mesoproterozoic activity evident in the exposed portions of the Namaqua–Natal Belt. Model depleted mantle dates from most of the lithologies analysed from the boreholes reflect a Palaeoproterozoic crustal history, similar to that evident in the Bushmanland and Richtersveld Sub-provinces of Namaqualand. This reworked Palaeoproterozoic crust is not evident in the Natal sector of the Namaqua–Natal Belt, nor in the Cape Meredith Complex, Falkland Islands, hence there must be a significant terrane boundary between the eastern (Natal) exposures and WE 1/66, the eastern-most borehole studied. Clearly, the Namaqua–Natal Belt formed by the accretion of isotopically distinct terranes during the Mesoproterozoic and reconstructions of the belt and its easterly extensions need to take this into account.

Acknowledgements

Jock Harmer is thanked for many fruitful discussions and Elijah Nkosi for helping to prepare the samples and mineral separates. Dave Reid and Maarten de Wit are thanked for their constructive suggestions whilst refereeing the manuscript.

References

Allen, R.B., Tucholke, B.E., 1981. Petrography and implications of continental rocks from the Agulhas Plateau, southwest Indian Ocean. Geology 9, 463–468.

Barton, E.S., 1983. The geochronology of the frontal zones of the Namaqua–Natal Mobile Belt. Ph.D. thesis (unpublished), University of Witwatersrand.

Burger, A.J., Coertze, F.J., 1973. Radiometric age measurements on rocks from southern Africa to the end of 1971. Bull. Geol. Surv. S. Afr. 58, 46–46.

Claoue-Long, J.C., Compston, W., Roberts, J., Fanning, C.M., 1995. Two Carboniferous ages: A comparison of SHRIMP

zircon dating with conventional zircon ages and $^{40}Ar/^{39}Ar$ analysis. SEPM Special Publication 54, 3–21.

Clifford, T.N., Barton, E.S., Retief, E.A., Rex, D.C., Fanning, C.M., 1995. A crustal progenitor for the intrusive anorthosite-charnockite kindred of the cupriferous Koperberg Suite O'kiep district. Namaqualand. J. Petrol. 36, 231–258.

Compston, W., Williams, I.S., Meyer, C., 1984. U–Pb geochronology of zircons from lunar breccia 73217 using a sensitive high mass-resolution ion microprobe. J. Geophys. Res. 89, B525–B534.

Cumming, G.L., Richards, J.R., 1975. Ore lead isotope ratios in a continuously changing earth. Earth Planet. Sci. Lett. 28, 155–171.

DePaolo, D.J., Linn, A.M., Schubert, G., 1991. The continental crustal age distribution: Methods of determining mantle separation ages from Sm–Nd isotopic data and application to the southwestern United States. J. Geophys. Res. 96, 2071–2088.

Eglington, B.M., Harmer, R.E., 1993. A review of the statistical principles of geochronometry: II. Additional concepts pertinent to radiogenic U–Pb studies. S. Afr. J. Geol. 96, 9–21.

Eglington, B.M., Harmer, R.E., 1999. GEODATE for Windows version 1: Isotope regression and modeling software. Counc. Geosci. Open File Rep. 206, 1–51.

Eglington, B.M., Harmer, R.E., Kerr, A., 1989. Isotope and geochemical constraints on Proterozoic crustal evolution in south-eastern Africa. Precambr. Res. 45, 159–174.

Grantham, G.H., Groenewald, P.B., Hunter, D.R., 1988. Geology of the northern H.U. Sverdrupfjella, western Dronning Maud Land and implications for Gondwana reconstructions. S. Afr. T. Nav. Antarkt. 18, 2–10.

Harmer, R.E., Lee, C.A., Eglington, B.M., 1998. A deep mantle source for carbonatite magmatism: Evidence from the nephelinites and carbonatites of the Buhera district, SE Zimbabwe. Earth Planet. Sci. Lett. 158, 131–142.

Hoal, B.G., Harmer, R.E., Eglington, B.M., 1989. Isotopic evolution of the Middle to Late Proterozoic Awasib Mountain Terrain in southern Namibia. Precambr. Res. 45, 175–189.

Jacobs, J., Thomas, R.J., Armstrong, R.A., Henjes-Kunst, F., 1999. Age and thermal evolution of the Mesoproterozoic Cape Meredith Complex, West Falkland. J. Geol. Soc. Lond. 156, 917–928.

Ludwig, K.R., 1998. On the treatment of concordant uranium-lead ages. Geochim. Cosmochim. Acta 62, 665–676.

Nicolaysen, L.O., Burger, A.J., 1965. Note on an extensive zone of 1000 million-year old metamorphic and igneous rocks in Southern Africa. Sciences de la Terre 10, 487–516.

Reid, D.L., 1997. Sm–Nd age and REE geochemistry of Proterozoic arc-related igneous rocks in the Richtersveld Subprovince, Namaqua Mobile Belt, Southern Africa. J. Afr. Earth Sci. 24, 621–633.

Reid, D.L., Smith, C.B., Watkeys, M.K., Welke, H.J., Betton, P.J., 1997. Whole rock radiometric age patterns in the Aggeneys-Gamsberg ore district Central Bushmanland South Africa. S. Afr. J. Geol. 100, 11–22.

Robb, L.J., Armstrong, R.A., Waters, D.J., 1999. The history of granulite-facies metamorphism and crustal growth from single zircon U–Pb geochronology: Namaqualand, South Africa. J. Petrol. 40, 1747–1770.

Rogers, N.W., Hawkesworth, C.J., 1982. Proterozoic age and cumulate origin for granulite xenoliths, Lesotho. Nature 299, 409–413.

Steiger, R.H., Jäger, E., 1977. Subcommission on geochronology: Convention on the use of decay constants in geo- and cosmochronology. Earth Planet. Sci. Lett. 36, 359–362.

Thomas, R.J., De Beer, C.H., Bowring, S.A., 1996. A comparative study of the Mesoproterozoic late orogenic porphyritic granitoids of southwest Namaqualand and Natal, South Africa. J. Afr. Earth Sci. 23, 485–508.

Thomas, R.J., Eglington, B.M., 1990. A Rb–Sr, Sm–Nd and U–Pb zircon isotopic study of the Mzumbe suite, the oldest intrusive granitoid in southern Natal, South Africa. S. Afr. J. Geol. 93, 761–765.

Thomas, R.J., Eglington, B.M., Bowring, S.A., Retief, E.A., Walraven, F., 1993. New isotope data from a Neoproterozoic porphyritic granitoid-charnockite suite from Natal, South Africa. Precambr. Res. 62, 83–101.

Thomas, R.J., Jacobs, J., Eglington, B.M., 2000. Geochemistry and isotopic evolution of the Mesoproterozoic Cape Meredith Complex, West Falkland. Geol. Magn. 137, 537–553.

Wareham, C.D., Pankhurst, R.J., Thomas, R.J., Storey, B.C., Grantham, G.H., Jacobs, J., Eglington, B.M., 1998. Pb, Nd and Sr mapping of Grenville-age crustal provinces in Rodinia. J. Geol. 106, 647–659.

Winter, H.d.l.R., Venter, J.J., 1970. Lithostratigraphic correlation of recent deep boreholes in the Karroo-Cape Sequence. In: Second Gondwana Symposium, Proceedings and Papers. Geol. Soc. S. Afr., Johannesburg, 395–408.